Journal of Research of the National Bureau of Standards Vol. 49, No. 3, September 1952 Research Paper 2356

Hydraulic Resistance Effect Upon the Dam-Break Functions*

Robert F. Dressler

The dam-break solution, a known centered simple-wave when resistance is neglected, is studied with the Chezy resistance formula added to the nonlinear shallow-water equations. Resistance transforms the wavefront from a characteristic curve into an envelope of characteristics. The flow near the tip differs from the other parts, due to a distinct boundary-layer type of region adjacent to the wavefront envelope. Then a perturbation leads to a system of partial differential equations with variable coefficients. Initial conditions are derived for the singularity at the origin. By studying its characteristic equations, this system is solved explicitly for the correction functions. Except at the tip, resistance raises the water surface and lowers velocities. These functions, no longer simple-waves, possess concurrent straight characteristic lines that map into another set of the same type. The critical flow locus moves downstream, faster for more resistance, and discharge rates are reduced. The method fails in the tip layer because the asymptotic expansions for the first derivatives lose validity there. Estimates are made indirectly for the wavefront velocity by observing where the boundary-layer effect becomes predominant.

1. Introduction

Sudden destruction of a dam results in a highly unsteady flow, with a forward wave (the "positive" wave) advancing over a dry channel, and a back disturbance (the "negative" wave) propagating into the still water above the dam. We consider a two-dimensional problem, a horizontal stream bed, with initially no water below the dam and water at rest above the dam. An explicit solution to this problem was given in 1892 by Ritter [1][1] by applying certain general expressions of Saint Venant [2]. The equations used were the usual approximate ones involving small curvature, due to Saint Venant, often called the nonlinear shallow-water equations.

The problem under consideration possesses genuine practical significance, not merely for the applications involving dynamiting of dams through military action, for example, the destruction in 1941 by Russian engineers of the Dnieprostroy Dam (140 feet high) near Kichkas on the Dnieper River, and the occasional mechanical failure, for example, the St. Francis Dam (205 feet high) in California, which broke in 1928 because of defective geologic foundations, causing the loss of hundreds of lives and immense property damage, but also for the more common occurrences, such as the opening of canal and sluice gates and controls at hydroelectric stations. The problem is most important, however, because of the information desired about the basic question of the behavior of any wave advancing along a dry channel, concerning which very little work has been done so far.

In the case of a wave advancing into still water of appreciable depth, the problem can be handled by approximating the flow with the discontinuity conditions of mass, momentum, and energy for a bore. In that case, one evaluates the relation between hydrostatic forces and rate of change of momentum at the wavefront. For our present case, however, this is not possible; rather, the controlling factor in the propagation of the wave is the hydraulic resistance caused by stream bed friction and turbulence. This effect will predominate especially in the shallow front region of the flow. For this reason the classical solution of Ritter, which neglects resistance, is not realistic. It should, therefore, be significant to initiate some study on the effects of resistance upon this unsteady flow. Forchheimer [3] has presented a summary of most previous work on the dam-break problem.

The experiments of Schoklitsch [4] indicate that actual velocities for the forward wave may be as low as 40 percent of the theoretical result given by Ritter's solution without resistance, whereas the experimental and theoretical results agree for the tip of the negative wave. Thus it is clear that the forward part of the flow is highly sensitive to hydraulic resistance, and it is our present purpose to deduce some approximate quantitative information of this effect by considering the equations containing the resistance term. Experiments of Eguiazaroff [5] likewise confirm the above observations; in his report, the author remarks about the almost complete absence of data concerning the propagation of a wave over dry land.

One can determine analytically the exact wavefront velocity (neglecting resistance) for the case where the bottom is inclined below the horizontal. We will study here, however, only the horizontal case, since the resistance predominates over the slope effect for the usual small slopes occurring in nature. Both effects could be handled simultaneously by the present approach, but since it is only the resistance term that seriously complicates the equations, the slope will be ignored.

In 1946 Ré [6] computed, by a finite-difference calculation on the characteristic equations, the flow to be expected from the destruction of a dam, for one specific value of slope and Chezy resistance coefficient. This was done in anticipation of possible destruction of a dam at the German-Swiss frontier in World War II. Ré's problem included the presence of some water below the dam initially, causing the formation of a bore in his solution.

* The preparation of this paper was sponsored (in part) by the Office of Naval Research.

[1] Figures in brackets indicate the literature references at the end of this paper.

2. The Basic Equations

We first define the problem in dimensional quantities (denoted by bars) and then transform immediately to dimensionless variables (unbarred). Let $\overline{Y}$ denote the height of the dam, and let the horizontal direction downstream from the dam be measured by $\overline{x}$. Upstream the water is at rest until time $\overline{t}=0$. Let $\overline{y}$ be the vertical distance of the water surface above the bed and $\overline{u}$ the horizontal component of velocity. Introducing $\overline{c}=\sqrt{g\overline{y}}$, the momentum and continuity equations used are

$$\frac{\partial \overline{u}}{\partial \overline{t}}+\overline{u}\frac{\partial \overline{u}}{\partial \overline{x}}+2\overline{c}\frac{\partial \overline{c}}{\partial \overline{x}}+\overline{R}\left(\frac{\overline{u}}{\overline{c}}\right)^2=0,$$

$$\overline{c}\frac{\partial \overline{u}}{\partial \overline{x}}+2\frac{\partial \overline{c}}{\partial \overline{t}}+2\overline{u}\frac{\partial \overline{c}}{\partial \overline{x}}=0, \tag{1}$$

containing the Chezy resistance term, in which the roughness coefficient $\overline{R}$ has dimensions of acceleration. Neglecting resistance, the well-known Ritter solution is

$$\overline{u}^0=\frac{2}{3}\left(\frac{\overline{x}}{\overline{t}}+\overline{H}\right)$$

$$\overline{c}^0=\frac{1}{3}\left(2\overline{H}-\frac{\overline{x}}{\overline{t}}\right), \tag{2}$$

where $\overline{H}=\sqrt{g\overline{Y}}$. This defines the parabolic surface profile for any fixed $\overline{t}$, with the negative wave propagating upstream at velocity $-\sqrt{g\overline{Y}}$, and the forward wave advancing at velocity $2\sqrt{g\overline{Y}}$. This profile always intersects the line $\overline{x}=0$ at height $\overline{y}=(4/9)\ \overline{Y}$ with $\overline{u}=(2/3)\ \overline{H}$, giving the constant discharge rate $\overline{Q}=\overline{u}\,\overline{y}=(8/27)\ (\overline{H}^3/g)$. The wave tip at $\overline{c}=\overline{y}=0$ has a horizontal tangent at all times, whereas it is known experimentally that the wavefront is actually vertical.

Transforming to dimensionless notation by the relations

$x=(g/\overline{H}^2)\overline{x}$, $t=(g/\overline{H})\overline{t}$, $u=\overline{u}/\overline{H}$, $y=\overline{y}/\overline{Y}$, $c=\overline{c}/\overline{H}$, $R=\overline{R}/g$, $Q=(g/\overline{H}^3)\ \overline{Q}$, and $m=x/t$, the equations become

$$\frac{\partial u}{\partial t}+u\frac{\partial u}{\partial x}+2c\frac{\partial c}{\partial x}+R\left(\frac{u}{c}\right)^2=0,$$

$$c\frac{\partial u}{\partial x}+2\frac{\partial c}{\partial t}+2u\frac{\partial c}{\partial x}=0, \tag{3}$$

for which the Ritter solution at $R=0$ becomes

$$u^0=\frac{2}{3}\left(\frac{x}{t}+1\right),$$

$$c^0=\frac{1}{3}\left(2-\frac{x}{t}\right). \tag{4}$$

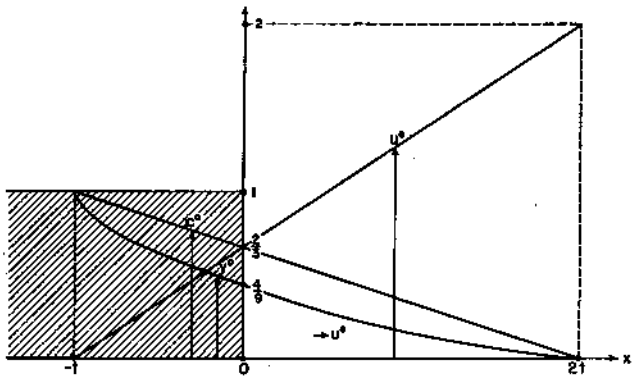

FIGURE 1. *Diagram of the Ritter solution.*

At the site, $x=0$, $y=4/9$, $u=2/3$, and $Q=8/27$ (fig. 1).

The characteristic equations equivalent to system (3), when $R=0$, are

$$I_+:\frac{dx}{dt}=u^\circ-c^\circ,$$

$$I_-:\frac{dx}{dt}=u^\circ+c^\circ,$$

$$II_+:d(u^\circ-2c^\circ)=0, \tag{5}$$

$$II_-:d(u^\circ+2c^\circ)=0,$$

defining two families γ_+ and γ_- of characteristic curves, along which the corresponding relations given above must hold. A study of these equations produces the Ritter solution by utilizing the solutions for the characteristic curves, which are

$$\gamma_+:x=mt,$$

$$\gamma_-:x=2t-3a^{2/3}t^{1/3}, \tag{6}$$

where m and a are parameters. The γ_- curves pass through the points $(-a,\ a)$. Since the γ_+ curves are concurrent straight lines through the origin in the x, t plane, the Ritter solution exemplifies what is now commonly called a "centered simple-wave." This simple-wave interpretation of the dam-break solution is discussed in Courant-Friedrichs [7] and Stoker [8]. Figure 2, A, shows the familiar pattern of characteristics for this solution given by (4), (5), and (6). Line OB marks the propagation of the disturbance into the still water, while OF is the trajectory of the forward wavefront, along which $c^\circ=0$. Therefore by (5) the two characteristic directions coincide along OF, which must belong to both the γ_+ and γ_- families. This means the solution of (3) with $R=0$ degenerates from hyperbolic to parabolic type along the boundary defined by the forward wavefront double characteristic.

As the resistence R changes from zero to a positive value, it will distort all the characteristics lying to the right of OB, as shown qualitatively in figure 2, B.

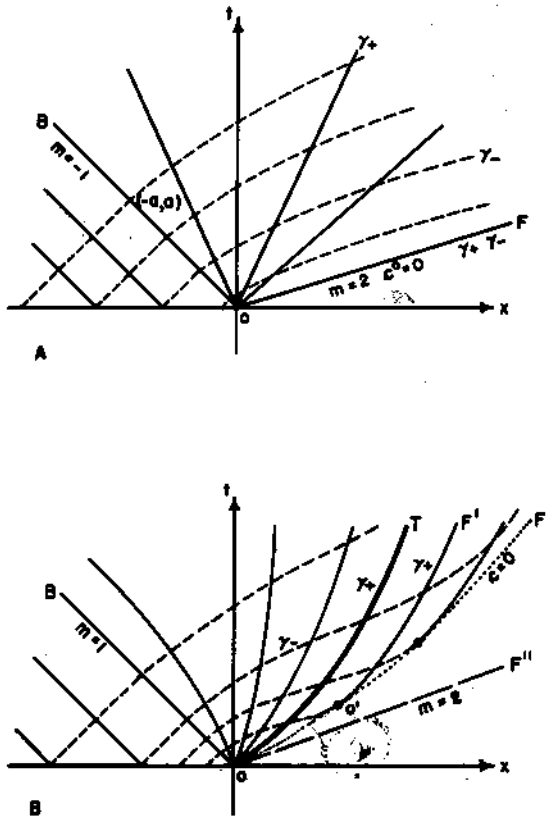

FIGURE 2. *Pattern of characteristics.*
A, Without resistance; B, with resistance.

The characteristic equations for R>0 become

$$I_+: \frac{dx}{dt} = u - c, \qquad I_-: \frac{dx}{dt} = u + c, \tag{7}$$

$$II_+: c^2(u-2c)_\alpha = -Ru^2 t_\alpha, \qquad II_-: c^2(u+2c)_\beta = -Ru^2 t_\beta, \tag{8}$$

introducing characteristic parameters α and β, which vary along γ_+ and γ_-, respectively. Equations (8) can be written in simpler notation as

$$II_+: d(u-2c) = -R\left(\frac{u}{c}\right)^2 dt, \qquad II_-: d(u+2c) = -R\left(\frac{u}{c}\right)^2 dt. \tag{9}$$

The characteristics for this solution in the region of motion are now unknown. In the still-water region upstream where $u \equiv 0$, γ_+ and γ_- have slopes $dx/dt = \mp 1$, respectively; hence they become straight lines here. Because the disturbance emanating from the origin will be carried as a derivative discontinuity along a γ_+ curve from (0, 0), on this curve we still have $u=0$, $c=1$, and therefore OB remains straight with slope -1. Resistance will decrease the forward wave velocity, turning the wavefront curve OF above the straight line $m=2$.

If R has any nonzero value, however small, it is seen in (3) that certain terms must become infinite at the wavefront, where $c=0$, to maintain the equality. It is experimentally known, or can be seen from these equations, that $c_x \to -\infty$ at the tip, that is, a vertical wavefront is maintained. Likewise, $c_t \to +\infty$, while u, u_x, and u_t remain bounded. This singular behavior of these derivatives will cause complications in the subsequent analysis. If the variable hydraulic radius were not present in the denominator of the resistance term, the entire problem would be basically simpler. In a somewhat similar way, it is this variable denominator that produces instability in a uniform flow and creates the possibility of roll-wave formation (see [9] and [10].)

The eq (3) used here are based upon hydrostatic pressure (negligible vertical accelerations or streamline curvature), and the question arises concerning their validity to describe the flow in the tip region. With $c_x \to -\infty$, the profile curvature becomes large, but the depth of water becomes zero, so that their product for the actual flow may stay small. Friedrichs [11] has shown that eq (3) apply when this product is small. Alternatively, one sees from experiment that the wave tip moves along somewhat like a separate mass of nearly fixed shape, with vertical accelerations therefore possibly negligible. In any case we wish to study the mathematical implications of (3) when applied to the dam-break problem.

In order to justify why the characteristic pattern should be as shown in figure 2, B, we will consider the following argument. Let the wavefront OF be defined as the locus, where $c=0$. It is implicit in the basic eq (3) that particles at the tip always remain at the tip, hence the velocity, u, evaluated along OF must always equal the reciprocal slope dx/dt of the line OF. Each of eq (7) is then satisfied by the wavefront curve; and at every point of OF, both characteristic directions γ_+ and γ_- coincide with the direction of OF. This line cannot be a characteristic curve itself, however, since neither of relations (9) can hold along OF for any $R>0$. Therefore, it must be an envelope of γ_+ and γ_- curves (fig. 2, B). Since the reflected γ_+ curves of class O′F′ cannot intersect each other, they must approach some limit line OT as O′→O. Three patterns therefore arise: (a) OT coincides with OB, (b) OT lies in the interior of section BOF, entering O at some intermediate angle between OB and OF, (c) OT is interior to BOF and enters O at the same angle as OF and OF″. Case (c) is shown in figure 2, B, because the following discussion indicates that (a) and (b) are not possible. We assume that the dam-break functions u (x, t, R) and c (x, t, R) are continuous in R at $R=0$ (but not necessarily so for their derivatives). Then the characteristic directions given by (7) will be continuous in R, and their curves must distort continuously as $R \to 0$.

If we transform to new variables by $x=x^*/K$, $t=t^*/K$ with $u(x,t)=u^*(x^*,t^*)$, $c(x,t)=c^*(x^*,t^*)$, defining a radial stretching centered at the origin with constant magnification K, eq (3) transform to

$$\frac{\partial u^*}{\partial t^*}+u^*\frac{\partial u^*}{\partial x^*}+2c^*\frac{\partial c^*}{\partial x^*}+\left[\frac{R}{K}\right]\left(\frac{u^*}{c^*}\right)^2=0,$$

$$2\frac{\partial c^*}{\partial t^*}+2u^*\frac{\partial c^*}{\partial x^*}+c^*\frac{\partial u^*}{\partial x^*}=0.$$

These equations are identical (in the starred quantities) with (3) except for the resistance coefficient. Hence the effect of letting $K\to\infty$, R fixed, increasing the stretching, is equivalent to the effect on the original quantities when $R\to 0$. The characteristic pattern for $R>0$ must therefore approach by continuous radial stretching the known limit pattern for $R=0$ (fig. 2, A). This is possible only for case (c). The limit chracateristic OT can now be used as a definition for the beginning of the tip layer TOF and as the separation line for this boundary-layer effect.

To obtain some quantitative results, we let the unknown solutions u and c to eq (3) be represented as asymptotic expressions of form

$$\begin{aligned} u(x,t,R)&\sim u^0(x,t)+U(x,t)R+u^{(2)}R^2+\ \ldots \\ c(x,t,R)&\sim c^0(x,t)+C(x,t)R+c^{(2)}R^2+\ \ldots, \end{aligned} \tag{10}$$

where u^0, c^0 is given by (4). Because of the above remarks about $\partial c/\partial x$ and $\partial c/\partial t$ at the wave tip for any $R>0$, whereas $\partial c^0/\partial x$ and $\partial c^0/\partial t$ stay finite, it follows that the derived expansions $\partial c/\partial x\sim\partial c^0/\partial x+\ \ldots$, and $\partial c/\partial t\sim\partial c^0/\partial t+\ \ldots$, cannot remain valid in the neighborhood of the wave tip. That is, the perturbation procedure based upon (10) becomes singular near the line OF, and from this standpoint also we see that some type of boundary-layer complication must develop there. Therefore these calculations, using the correction functions U and C, cannot be applied directly to the wavefront layer.

Substituting (10) into (3) and equating terms independent of R produce eq (3) with $R=0$ and their solution (4). At the next step, using terms of first degree in R, the equations defining $U(x,t)$ and $C(x,t)$ become, by (4),

$$2\left(1+\frac{x}{t}\right)\frac{\partial U}{\partial x}+3\frac{\partial U}{\partial t}+2\left(2-\frac{x}{t}\right)\frac{\partial C}{\partial x}+\frac{2}{t}U-\frac{2}{t}C+3\left[\frac{1+\frac{x}{t}}{1-\frac{x}{2t}}\right]^2=0 \tag{11}$$

$$\left(2-\frac{x}{t}\right)\frac{\partial U}{\partial x}+4\left(1+\frac{x}{t}\right)\frac{\partial C}{\partial x}+6\frac{\partial C}{\partial t}-\frac{2}{t}U+\frac{2}{t}C=0.$$

In order to solve this nonhomogeneous system with variable coefficients, we will first derive the appropriate initial and boundary conditions and then study the associated characteristic equations.

3. Initial and Boundary Conditions for U, C

At the initial moment of breakage, the water height and the velocity are multivalued at $x=0$. This means that the full solution u, c with resistance has a singularity at the origin; the lowest order approximation u^0, c^0 possesses a singularity there also. Will there likewise be singularities in the higher order terms at (0, 0), or is the entire effect contained in u^0, c^0? In order to get the procedure started in his finite-difference calculations, Ré [6] assumed that the flow could be considered initially as two finite shocks, one positive and one negative. When our problem is considered as defined by (3) with $R>0$, since the velocity starts off discontinuously with nonzero values, the opposing force $-R(u/c)^2$ must become operative instantaneously. Although it has already been indicated that resistance effects on u and c can be ignored in the immediate neighborhood of the origin, a more detailed discussion will also be made now for the behavior of U and C there.

Let the limit values be u_i, c_i for the solutions u, c as we approach the origin along a curve with a limiting slope m_i. By (4),

$$\begin{aligned} u_i^0&=\frac{2}{3}m_i+\frac{2}{3}, \\ c_i^0&=\frac{2}{3}-\frac{1}{3}m_i. \end{aligned} \tag{12}$$

For example, as we approach (0, 0) along OB (fig. 2, A), $c_i^0=1$; along OF, $c_i^0=0$; and intermediate values result for an approach within region BOF. For all such approaches, by (12), $u_i^0+2c_i^0\equiv 2$ through the origin point, consistent with the characteristic relation $d(u^0+2c^0)=0$ for γ_- in (5). One may consider this origin point to be stretched out into a γ_- characteristic curve, with c^0 varying continuously from 1 to 0 along this curve from left to right.

Now going over to the full problem with $R>0$ (fig. 2, B), we likewise consider point O to be stretched into the arc MN, shown schematically in figure 3. Interpreting the curve MNF as a γ_- characteristic, the relation holding along it by (9) is

$$d(u+2c)=-R\left(\frac{u}{c}\right)^2dt \tag{13}$$

if $c\neq 0$; but $c=0$ only at N. Hence (13) is applicable on MN, along which $dt=0$. This means $u+2c$ is constant along MN, and so

$$u_i+2c_i=2. \tag{14}$$

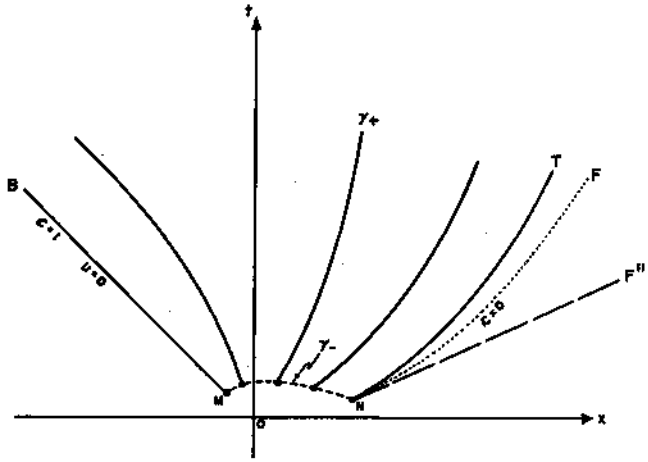

FIGURE 3. *Schematic diagram of characteristics at origin.*

Approaching MN along any γ_+ curve,

$$m_i=\lim \frac{dx}{dt}=u_i-c_i \tag{15}$$

by (7). The solution of (14) and (15) is

$$u_i=\frac{2}{3}\,m_i+\frac{2}{3},$$

$$c_i=\frac{2}{3}-\frac{1}{3}\,m_i, \tag{16}$$

Using (10), $u_i=\lim\ (u^0+U\ R+\ .\ .\ .)$, we obtain by (12)

$$U_i=0, \qquad C_i=0, \tag{17}$$

which are the desired conditions on U and C at the origin. This result shows that the resistance effects on the main solution can be ignored at the initial instant.

The relations $c(-t,t,R)\equiv 1$, $u(-t,t,R)\equiv 0$, previously discussed, give the necessary data for U and C along line OB. The use of these with (10) yields

$$C(-t,t)\equiv 0, \qquad U(-t,t)\equiv 0. \tag{18}$$

4. The Solution for U and C

To obtain a clue for solving most easily for U and C subject to the conditions just derived, we now study the characteristic equations equivalent to system (11), which are

$$\mathrm{I}_+ : \frac{dx}{dt}=u^0-c^0,$$

$$\mathrm{I}_- : \frac{dx}{dt}=u^0+c^0,$$

$$\mathrm{II}_+ : d(U-2C)=\left[\frac{4}{3t}(C-U)-\left(\frac{1+\frac{x}{t}}{1-\frac{x}{2t}}\right)^2\right]dt, \text{ if } \frac{x}{t}<2.$$

$$\mathrm{II}_- : d(U+2C)=-\left(\frac{1+\frac{x}{t}}{1-\frac{x}{2t}}\right)^2 dt, \text{ if } \frac{x}{t}<2. \tag{19}$$

The characteristics are the same as (6) for u^0, c^0 (fig. 2, A), but now the relations along them are more complicated. Relation II_- has the right side independent of the unknown, and can therefore be integrated along the γ_- curves, using (6) and (18). The resulting integral along γ_- becomes

$$\frac{U+2C}{a}=\frac{32}{35}-4\left(\frac{t}{a}\right)\left[\frac{3}{7}\left(\frac{t}{a}\right)^{4/3}-\frac{6}{5}\left(\frac{t}{a}\right)^{2/3}+1\right]. \tag{20}$$

This equation used with II_+ of (19) now indicates how to solve explicitly for U and C as follows.

If we move out from the origin along a straight γ_+ characteristic, the value of t at an intersection with a γ_- curve emanating from $(-a,\ a)$ must be proportional to a. This is immediately seen since the equations for the two curves can be written in the form $(x/a)=m\ (t/a)$ and $(x/a)=2(t/a)-3(t/a)^{1/3}$. Now by (20), the quantity $(U+2C)/a$ is a function of t/a, which is constant along each γ_+ ray. Therefore, $U+2C$ is also proportional to a along the ray, and so $U+2C$ must be proportional to t there. Next we observe in the II_+ relation of (19) that $U-2C$ would likewise be proportional to t along a γ_+ ray if the term $(4/3t)\ (C-U)$ were a constant there; then each of the quantities U and C would separately be proportional to t. But this would then be sufficient to make $(4/3t)(C-U)$ constant as required. Therefore the solutions U, C must actually be linear in t along each γ_+ ray, since this will also satisfy the condition (17) at the origin. With this information, the original system (11) can now be solved explicitly, subject to the other boundary condition along OB.

We transform to the new independent variables m and t, putting $C(x,t)=\tilde{C}(m,t)$ and $U(x,t)=\tilde{U}(m,t)$. Then (11) transforms to

$$\frac{2-m}{t}\frac{\partial\tilde{U}}{\partial m}+3\frac{\partial\tilde{U}}{\partial t}+\frac{2(2-m)}{t}\frac{\partial\tilde{C}}{\partial m}+\frac{2}{t}\tilde{U}-\frac{2}{t}\tilde{C}+3\left(\frac{1+m}{1-\frac{m}{2}}\right)^2=0,$$

$$\frac{2-m}{t}\frac{\partial\tilde{U}}{\partial m}+\frac{2(2-m)}{t}\frac{\partial\tilde{C}}{\partial m}+6\frac{\partial\tilde{C}}{\partial t}-\frac{2}{t}\tilde{U}+\frac{2}{t}\tilde{C}=0, \tag{21}$$

with $\tilde{U}(-1,t)\equiv\tilde{C}(-1,t)\equiv 0$ for condition (18). Introduction of $\tilde{U}=h(m)t$ and $\tilde{C}=k(m)t$ leads to the system

$$(2-m)\frac{dh}{dm}+5h+2(2-m)\frac{dk}{dm}-2k+3\left(\frac{1+m}{1-\frac{m}{2}}\right)^2=0,$$

$$(2-m)\frac{dh}{dm}-2h+2(2-m)\frac{dk}{dm}+8k=0. \tag{22}$$

This possesses the solution, for $h(-1)=k(-1)=0$,

$$h(m)=-\frac{108}{7(2-m)^2}+\frac{12}{2-m}-\frac{8}{3}+\frac{8\sqrt{3}}{189}(2-m)^{3/2},$$

$$k(m)=\frac{6}{5(2-m)}-\frac{2}{3}+\frac{4\sqrt{3}}{135}(2-m)^{3/2}. \tag{23}$$

The desired quantities U, C are then given by ht, kt, respectively.

The characteristic eq (19) have thus furnished an easy method for obtaining the particular solution U, C. It would have been possible, however, to solve the original system (11) first for its general solution, but with much more difficulty. This general solution to (11) is

$$U(x,t)=-\frac{2}{t}\Psi\left(\frac{x}{t}\right)-\left(\frac{108}{7\left(2-\frac{x}{t}\right)^2}-\frac{12}{2-\frac{x}{t}}+\frac{8}{3}\right)t+\Phi(\tau),$$

$$C(x,t)=\frac{1}{t}\Psi\left(\frac{x}{t}\right)+\left(\frac{6}{5\left(2-\frac{x}{t}\right)}-\frac{2}{3}\right)t+$$

$$\frac{\delta}{\tau}+\frac{1}{2}\Phi(\tau)+\frac{1}{2\tau}\int^{\tau}\Phi(\xi)d\xi,$$

where Ψ and Φ are arbitary functions, δ is an arbitrary constant, and $\tau=(2-x/t)t^{2/3}$. In order to keep the corrections finite at the origin, one must select $\Psi\equiv 0$ and $\delta=0$. These expressions for the general solution indicate in an alternative manner the correctness of our conditions (17) at the origin, since we can now see that no other finite values except $U_i=C_i=0$ could be prescribed there. Then conditions (18) along line OB require the selection $\Phi(\tau)=(8\sqrt{3}/189)(2-x/t)^{3/2}t$. The resulting particular solutions are seen to be identical with those previously given by (23).

These particular solutions U and C no longer define a centered simple-wave (as for u°, c° for which the maps of all the x, t characteristics fall on one Γ curve in the u, c plane), but rather define what might be called a "centered seimilinear wave". The map of its characteristics is shown in figure 4. For these solutions it is clear that the γ_+ straight lines in figure 2, A, must map into a pencil of straight lines Γ_+ through the origin (fig. 4). The γ_- family goes over into curves Γ_- (dotted in fig. 4) also concurrent at the origin. The line OB and the origin in the x, t plane map into the single point (0, 0) in the U, C plane. All of the curves remain inside the wedge formed by AO (with slope $-\frac{1}{2}$) and the negative U axis.

The dam-break solution with first order resistance correction is then

$$u(x,t,R)\sim\frac{2}{3}(1+m)+h(m)tR+\ \ldots,$$

$$c(x,t,R)\sim\frac{1}{3}(2-m)+k(m)tR+\ \ldots, \tag{24}$$

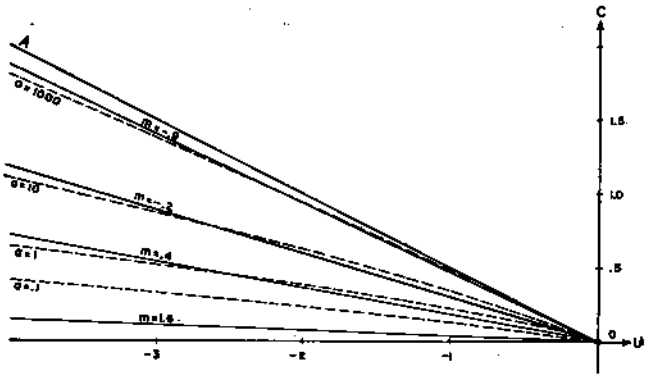

FIGURE 4. *Map of characteristics in U, C plane.*

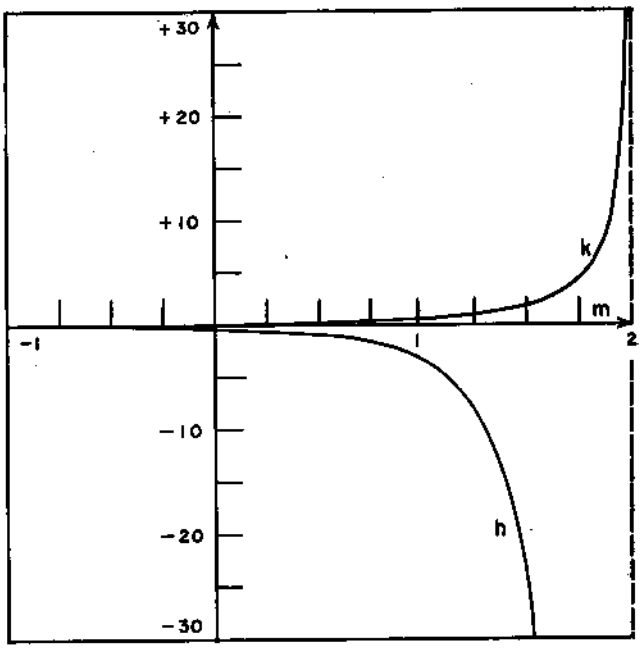

FIGURE 5.

with h, k defined in (23) and $m=x/t$. Up to first-order terms, the solutions depend only upon the product $tR=\sigma$. Both h and k have poles at $m=2$ due to the tip effect; the behavior of these functions is shown in figure 5. It is seen that resistance causes a much greater effect upon the velocity than upon c or the height, since $|h|$ greatly exceeds k.

For a fixed R, (23) implies that the value given by (24) for u must eventually become negative as we go far enough out from the origin along any γ_+ curve. Thus the asymptotic validity of our series weakens with increasing distance from the origin, as the U, C characteristics diverge further from the true characteristics of figure 2, B. For all numerical results presented here, the calculations have been restricted arbitrarily to a region comprising less than one-third the distance to the points where the series would indicate a zero value for u.

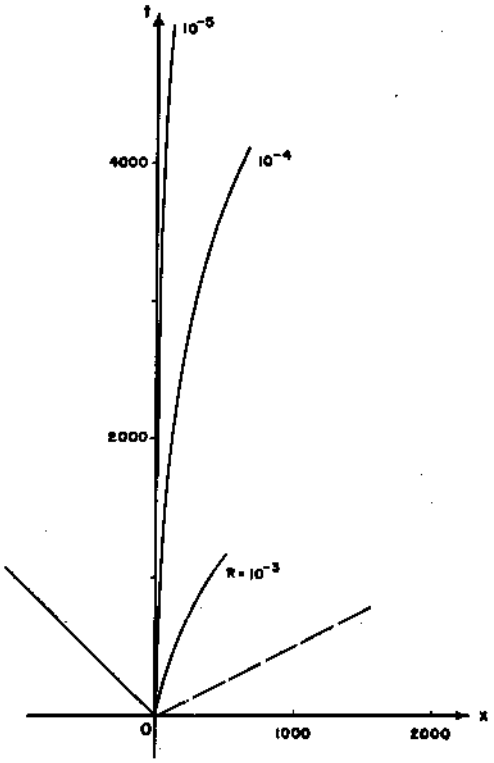

FIGURE 6. *Locus of critical flow.*

5. Locus of Critical Flow

In the u°, c° solution, the flow always remains critical (where $\bar{u}=\sqrt{g\bar{y}}$ or $u=c$) for all $t>0$ at $x=0$, with subcritical flow for $x<0$ and supercritical for $x>0$. The resistance will distort this critical flow locus. To calculate it, we denote the locus where $u=c$ by $x=s(t,R)\sim S(t)R+s^{(2)}(t)R^2+\ldots$, since $s^\circ(t)\equiv 0$. Using the relation $u(s[t,R],t,R)\equiv c(s[t,R],t,R)$ we obtain

$$u^\circ(s[t,R],t)+U(s[t,R],t)R+\ldots$$
$$\equiv c^\circ(s[t,R],t)+C(s[t,R],t)R+\ldots, \qquad (25)$$

and then expand each function in this identity in a series about $x=0$. Equating terms of first order in the resulting double series gives the result $S(t)=t[C(0,t)-U(0,t)]$. The equation of the locus of critical flow correct to first order is therefore the parabola

$$x=[k(0)-h(0)]Rt^2\doteq 0.395Rt^2. \qquad (26)$$

Figure 6 shows this locus for various values of R within extreme practical limits. We observe that the critical flow position moves continually downstream, and the resistance increases the proportion of the total flow which is subcritical.

We note parenthetically that this double series method cannot be utilized to obtain the locus of the wavefront because of the tip effect. If one designates by $x=z(t,R)$ the locus where $c=0$, with $z\sim 2t+\mathcal{Z}(t)\,R+\ldots$, and $u(z,t,R)\equiv z_t$, one would compute in this manner the formal results

$$\mathcal{Z}(t)=3tC(2t,t)=t^{2/3}\int_0^t U(2\tau,\tau)\tau^{-2/3}d\tau,$$

which are undefined in this case because of the singularities of U and C along the line $x=2t$.

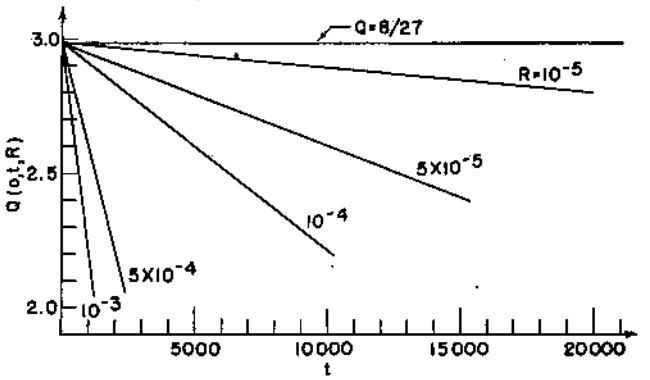

FIGURE 7. *Discharge rates.*

6. The Discharge Rate

From the dimensional discharge rate $\bar{Q}=\bar{u}\,\bar{y}$, we define $Q=(g/\bar{H}^3)\bar{Q}=u\,c^2$, the corresponding dimensionless quantity. For the discharge rate at the site of the dam,

$$Q(0,t,R)\doteq\left[\frac{2}{3}+U(0,t)R\right]\left[\frac{2}{3}+C(0,t)R\right]^2,$$

which becomes, after neglecting terms above first order,

$$Q(0,t,R)\doteq\frac{8}{27}(1-0.239tR). \qquad (27)$$

Figure 7 presents these data for various resistances.

7. Approximations for the Wavefront

We see from the experimental profiles obtained by Schoklitsch [4], converted into dimensionless form by Keulegan [12], figure 8, that the dam-break wave actually governed by resistance has a vertical slope at the tip. As previously discussed here, eq (3) shows that $|c_x|$ and $|y_x|$ become infinite when $c=0$. In the region where $|c_x|$ begins to grow large, our expansions lose validity and the present method of attack breaks down. To handle the tip region accurately, some type of boundary-layer technique would be necessary. This is being investigated at present, but no results are yet available. Figure 9 illustrates schematically this spearation of the two regions, with T marking the transition zone. For present purposes, this point T of transition will be described merely as a point where $|c_x|$ and $|y_x|$ begin to grow large rapidly.

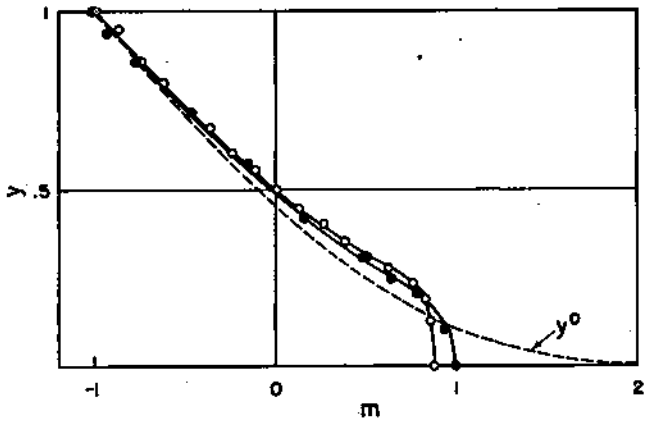

FIGURE 8. *Wave profiles according to Schoklitsch.*
● t=43; ○ t=109.

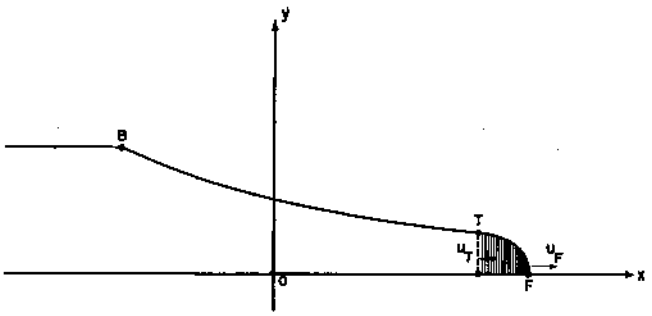

FIGURE 9. *Velocities in the wave tip.*

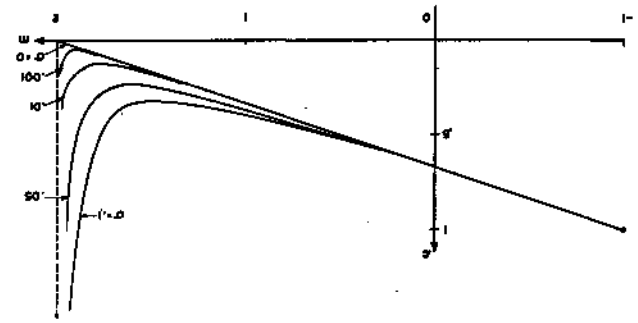

FIGURE 10.

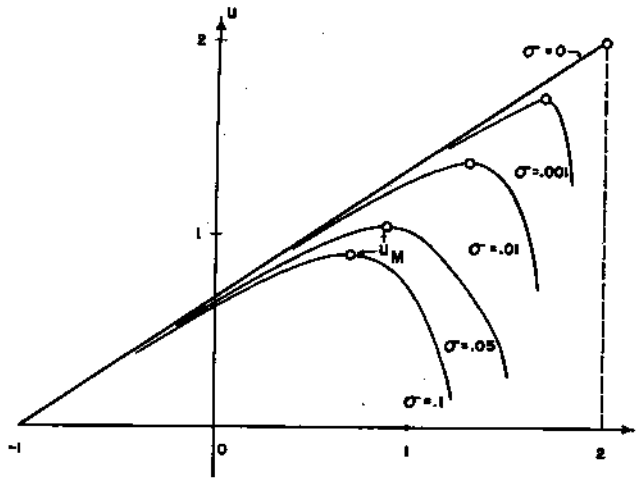

FIGURE 11.

In the absence of any more satisfactory boundary-layer results, we will apply the following approximate considerations to obtain some data about the wavefront. This rough method seems justifiable since there appear to be no other theoretical data and almost no experimental data available on this problem.

We visualize the tip region to be moving somewhat like a separate entity pushed along by the water behind it, and in the tip, u should be changing (increasing) rather slowly toward the front. Hence u_T could be taken as an approximation for u_F.

Next we make the following approximation for u_T. The results in (24) are graphed in figures 10 and 11. Each curve corresponds to a particular value of the parameter $\sigma=Rt$. The c curves, being based upon expressions that lose validity toward the tip, reach a minimum and then turn upward. Analogously, each u curve attains a maximum. Since the true values for c and u should not increase or decrease, respectively, toward the tip, these extremal points must lie already in the tip region. As estimates for u_T we will take u_M, the maximum values of u, indicated by the small circles in figure 11. Actually the tip region will begin before these maximum points are obtained, thus making the approximation too high; but if u_M is now taken as an approximation to u_F, since $u_T<u_F$, these effects will partly compensate for each other to improve the accuracy of the approximation. In figure 11 the locus of maximum points defines a function $\sigma(m)$. Using $\partial u(m,\sigma)/\partial m\equiv 0$, this relation is found to be

$$\sigma(m)=\left(6\left[\frac{54}{7(2-m)^3}-\frac{3}{(2-m)^2}+\frac{\sqrt{3}}{63}(2-m)^{\frac{1}{2}}\right]\right)^{-1}. \tag{28}$$

Using (24), the value $u_M=u(m(\sigma),\sigma)$ where $m(\sigma)$ is the inverse function in (28). Applying this as an estimate for the wavefront velocity, these values are graphed in figure 12 as functions of t, with R as a parameter over the limits of the practical range. All the curves must leave the point (2, 0) with vertical tangents.

To obtain the corresponding estimate for the trajectory of the wavefront, the velocity curves of figure 12 are integrated to give the position of the tip in the x,t plane, with R as parameter (fig. 13).

A series of experiments is contemplated here at the National Hydraulic Laboratory to check the validity of the analysis presented and to investigate in more detail the actual behavior of water particles at the tip of a positive wave advancing over a dry channel.

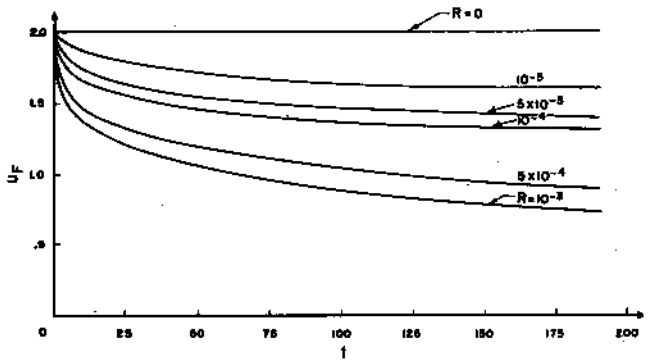

FIGURE 12. *Approximate wave-front velocity.*

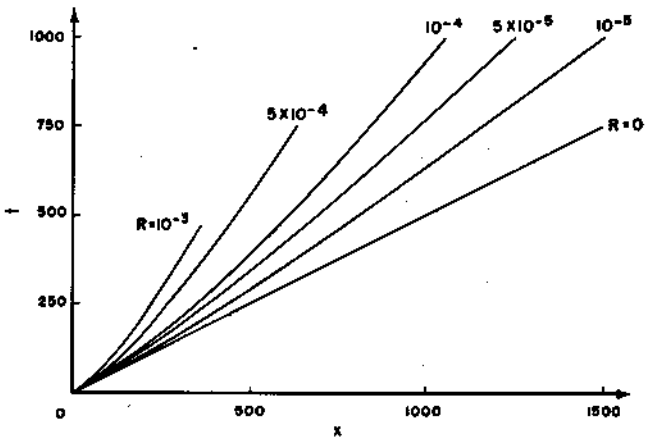

FIGURE 13. *Approximate wave-front trajectory.*

8. References

[1] A. Ritter, Die Fortpflanzung der Wasserwellen, Z. Ver. deut. Ing. **36** (1892).

[2] B. de Saint Venant, Théorie du movement non permanent des eaux, Compt. rend. **73** (1871).

[3] Philipp Forchheimer, Hydraulik, (Teubner, Leipzig, 1930).

[4] A. Schoklitsch, über Dambruchwellen, Sitzber. Akad. Wiss. Wien. **126** (1917).

[5] I. B. Eguiazaroff, Regulation of the water level in the reaches of canalized rivers, XVI International Congress of Navigation, Brussels (1935).

[6] Ré, Étude du lacher instantane d'une retenue d'Eau dans un canal par la méthode graphique, (La Houille Blanche, May 1946).

[7] R. Courant and K. O. Friedrichs, Supersonic flow and shock waves, (Interscience, New York, 1948).

[8] J. J. Stoker, Formation of breakers and bores, Communications on Applied Mathematics **I,** No. 1 (New York University, 1948).

[9] R. F. Dressler, Roll-waves in inclined open channels, Communications on Applied Mathematics **II,** No. 2/3 (New York University, 1949).

[10] R. F. Dressler, Stability of uniform flow and roll-wave formation, Symposium on Gravity Waves, NBS Circular 521 (in press).

[11] K. O. Friedrichs, On the derivation of the shallow-water theory, Appendix to Stoker paper [8].

[12] G. H. Keulegan, Engineering hydraulics, Chapter XI on wave motion (John Wiley & Sons, New York, N. Y. 1950).

Washington, May 28, 1952.